Very High-Energy Gamma-Ray Observations of PSR B1509−58 with the CANGAROO 3.8m Telescope

T. Sako [1,14], Y. Matsubara [1], Y. Muraki [1], P. V. Ramanamurthy [1], S. A. Dazeley [2], P. G. Edwards [3], S. Gunji [4], T. Hara [5], S. Hara [6], J. Holder [7,15], S. Kamei [6], A. Kawachi [7], T. Kifune [7], R. Kita [8], A. Masaike [9], Y. Mizumoto [10], M. Mori [7], M. Moriya [6], H. Muraishi [8], T. Naito [10], K. Nishijima [11], S. Ogio [6], J. R. Patterson [2], G. P. Rowell [7], K. Sakurazawa [6], Y. Sato [7], R. Susukita [12], R. Suzuki [6], T. Tamura [13], T. Tanimori [6], G. J. Thornton [2], S. Yanagita [8], T. Yoshida [8] and T. Yoshikoshi [7]

Received _____; accepted _____

[1] Solar-Terrestrial Environment Laboratory, Nagoya University, Nagoya 464-8601, Japan

[2] Department of Physics and Mathematical Physics, University of Adelaide, South Australia 5005, Australia

[3] Institute of Space and Astronautical Science, Sagamihara 229-8510, Japan

[4] Department of Physics, Yamagata University, Yamagata, Yamagata 990-8560, Japan

[5] Faculty of Management Information, Yamanashi Gakuin University, Kofu 400-8575, Japan

[6] Department of Physics, Tokyo Institute of Technology, Tokyo 152-8551, Japan

[7] Institute for Cosmic Ray Research, University of Tokyo, Tokyo 188-8502, Japan

[8] Faculty of Science, Ibaraki University, Mito 310-8521, Japan

[9] Department of Physics, Kyoto University, Kyoto 606-8502, Japan

[10] National Astronomical Observatory of Japan, Tokyo 181-8588, Japan

[11] Department of Physics, Tokai University, Hiratsuka 259-1292, Japan

[12] Institute of Physical and Chemical Research, Wako 351-0198, Japan

[13] Faculty of Engineering, Kanagawa University, Yokohama 221-8686, Japan

[14] present address; LPNHE, Ecole Polytechnique, Palaiseau CEDEX 91128, France; sako@poly.in2p3.fr

[15] present address; LAL, Universite de Paris-Sud, BP 34, ORSAY CEDEX 91898, France

ABSTRACT

The gamma-ray pulsar PSR B1509−58 and its surrounding nebulae have been observed with the CANGAROO 3.8m imaging atmospheric Čerenkov telescope. The observations were performed from 1996 to 1998 in Woomera, South Australia, under different instrumental conditions with estimated threshold energies of 4.5 TeV (1996), 1.9 TeV (1997) and 2.5 TeV (1998) at zenith angles of $\sim 30°$. Although no strong evidence of the gamma-ray emission was found, the lowest energy threshold data of 1997 showed a marginal excess of gamma-ray–like events at the 4.1 σ significance level. The corresponding gamma-ray flux is calculated to be $(2.9 \pm 0.7) \times 10^{-12}\,\mathrm{cm}^{-2}\mathrm{s}^{-1}$ above 1.9 TeV. The observations of 1996 and 1998 yielded only upper limits (99.5% confidence level) of $1.9 \times 10^{-12}\,\mathrm{cm}^{-2}\mathrm{s}^{-1}$ above 4.5 TeV and $2.0 \times 10^{-12}\,\mathrm{cm}^{-2}\mathrm{s}^{-1}$ above 2.5 TeV, respectively. Assuming that the 1997 excess is due to Very High-Energy (VHE) gamma-ray emission from the pulsar nebula, our result, when combined with the X-ray observations, leads to a value of the magnetic field strength $\simeq 5$ μG. This is consistent with the equipartition value previously estimated in the X-ray nebula surrounding the pulsar. No significant periodicity at the 150 ms pulsar period has been found in any of the three years' data. The flux upper limits set from our observations are one order of magnitude below previously reported detections of pulsed TeV emission.

Subject headings: gamma-rays: observations — pulsars: individual (PSR B1509−58) — supernova remnants

1. Introduction

Pulsar nebulae have been suggested as a possible acceleration site of high-energy particles in the galaxy (Harding 1990). The first order Fermi acceleration mechanism is expected to occur in a shock between the pulsar wind and supernova ejecta, or interstellar matter. Evidence of such energetic phenomena has been obtained through observation of synchrotron emission by accelerated electrons and positrons at radio to gamma-ray ($\leq$ 10 GeV) energies. However, more direct evidence has become obtainable through Very High-Energy (VHE) gamma-ray ($\geq$ 300 GeV) observations over the last decade using the Imaging Atmospheric Čerenkov Technique (IACT).

VHE gamma-ray emissions from the directions of three energetic pulsars, the Crab (Weekes et al. 1989; Vacanti et al. 1991; Tanimori et al. 1994); the Vela pulsar (Yoshikoshi et al. 1997) and PSR B1706−44 (Kifune et al. 1995, Chadwick et al. 1997), have been detected by ground-based telescopes using the IACT. Although all three pulsars show pulsed emission in the *EGRET* energy range (100MeV–10GeV), none of the VHE gamma-ray detections have shown any periodicity at the radio pulsar period. This steady VHE gamma-ray emission is usually explained to be a result of the inverse Compton scattering in the pulsar nebula, and not from the pulsar magnetosphere. While the mechanism of the emission from the Crab nebula is well studied (see, for example, de Jager et al. 1996), information on other pulsars is still sparse. In order to study pulsars and their surrounding environment as possible acceleration sites of the cosmic rays, more examples in the VHE gamma-ray range are required.

PSR B1509−58 was discovered as an X-ray pulsar by Seward and Harnden (1982) using the *Einstein X-ray Observatory.* It is near the center of the supernova remnant MSH15−52 (G320.4−1.2). Soon after this discovery, pulsed radio emission was found by Manchester, Tuohy and D'Amico (1982). The pulsar has a period of 150 msec and a period derivative of

1.5 $\times 10^{-12}$ ss^{-1}, the largest known today. The characteristic age of the pulsar is estimated to be ~1700 years (Manchester et al. 1998), which makes it the second youngest pulsar after the Crab. [1] From the period and the large period derivative, a very strong surface magnetic field of 1.5×10^{13} G and a large spin down energy loss rate of 1.8×10^{37} ergs s^{-1} are implied. While the distance to the pulsar is relatively large (4.4 kpc, Taylor et al. 1995), the expected energy flux received at the Earth is the fifth largest among the known pulsars.

A compact ($\sim 10' \times 6'$) synchrotron X-ray nebula has been found to exist around PSR B1509−58 (Seward et al. 1984). The synchrotron emission suggests the existence of non-thermal electrons (positrons) in the nebula, which will also emit VHE gamma-rays via inverse Compton scattering. A detectable VHE gamma-ray flux from this synchrotron nebula was predicted by du Plessis et al. (1995) as a function of the magnetic field strength in the nebula. The expected gamma-ray flux above 1 TeV of 10^{-11} to $10^{-12}\,cm^{-2}s^{-1}$ for nebula magnetic fields 4 to 10 μG is within the sensitivity of the CANGAROO 3.8m telescope. Thus, VHE observations should give a good measurement of the magnetic field strength of this nebula. Du Plessis et al. (1995) also predicted a very hard differential spectral index of ~1.8 based on the X-ray observations. This prediction provides us with an extreme example of the utility of multiwavelength studies of synchrotron—inverse-Compton emitting objects. Besides the compact nebula, recent X-ray satellite observations suggest various non-thermal phenomena in this remnant. *ROSAT* observations indicate a non-thermal X-ray component from the central diffuse nebula (CDN) extending to a diameter of $50'$ ($\sim$ 60pc) centered on the pulsar (Trussoni et al. 1996). *ASCA* observations

[1] Torii et al. (1997) have reported the discovery of a pulsar 1600 years old. This age is somewhat speculative however as the period derivative of the pulsar has not yet been measured and an association with a historical supernova was assumed to estimate the pulsar age.

revealed a non-thermal jet structure between the pulsar and the center of a thermal nebula about 10′ north from the pulsar (Tamura et al. 1996). In order to explain the effective thermalization process of the thermal nebula, Tamura et al. (1996) indicate the existence of accelerated ions as well as electrons in the jet. Furthermore, Gaensler et al. (1998) found synchrotron emission from compact knots in this thermal nebula from 20cm imaging observations with the Australia Telescope Compact Array.

The surface magnetic field strength of the pulsar PSR B1509−58 is estimated to be one of the largest among known pulsars. Due to the photon splitting process caused by this strong surface magnetic field, a cut-off in the pulsed emission around MeV energies is predicted by Harding, Baring and Gonthier (1997). In fact, Kuiper et al. (1999) have suggested that a cut-off around 10 MeV exists in the *COMPTEL* data. *EGRET* observations have resulted in only an upper limit for the pulsed emission from PSR B1509−58 (Thompson et al. 1994). In contrast, Nel et al. (1992) have reported the detection of transient pulsed VHE gamma-rays from the observations between 1985 and 1988 based on ground–based (non-imaging) Čerenkov telescope observations. However they could not detect any significant pulsed emission in the successive years. They tried to explain their observations with the framework of the outer gap model (Cheng, Ho and Ruderman 1986). (Bowden et al. (1993) reported a upper limit of the pulsed emission above 0.35 TeV from their observations in 1987 and 1989. Combining with the detection by Nel et al. (1992) in 1987 above 1.5 TeV, power law index of the integral energy spectrum is limited to be harder than ~ 1.) Interestingly, Kuiper et al. (1999) also indicate a marginal detection of the pulsed emission above 10 MeV, where the origin may differ from that at lower energies. Consequently, we have examined our data for the presence of periodicity as well. Our observations are the first results on this pulsar with using the IACT, which is one order of magnitude more sensitive than non-imaging observations.

For the reasons given above, we believed that PSR B1509−58 would be an interesting object to study above 1 TeV energies with the CANGAROO 3.8m IACT telescope in both the steady nebula emission and the pulsed emission. Details of those observations are given in Section-2. The methods of the analysis and results are shown in Section-3. In Section-4, we summarize our results and discuss their implications.

2. Observations

The CANGAROO (Collaboration between Australia and Nippon (Japan) for a GAmma-Ray Observatory in the Outback) 3.8m telescope is located at Woomera, South Australia (136°47′E, 31°6′S and 160m a.s.l.). Čerenkov photons emitted from extensive air showers originated by primary gamma-rays and cosmic rays are collected with a parabolic mirror of 3.8m diameter and detected with an imaging camera at the focal plane. The camera consists of 256 photomultiplier tubes (PMTs) of 10mm×10mm size (Hamamatsu R2248). The PMTs are located in a 16×16 square grid and the field of view amounts to 3°× 3°. When signals from more than 5 tubes exceed 3 photoelectrons each within a gate, a trigger is generated. The amplitude and relative time of each PMT signal, the event time, and the counting rate of each tube are recorded for each event. The absolute time can be obtained with a precision of 200 nsec using a GPS clock. In addition to the GPS clock, the time of a crystal clock with a precision of 100μsec is also recorded. The GPS clock was not available in the 1997 observations due to the installation work of our new data acquisition system. However, because the time indicated by the crystal clock shows a stable drift from that of the GPS clock, we can obtain accurate *relative* arrival times for events even without the GPS clock. The crystal clock is reset every observation (new moon) period. Therefore, a periodicity analysis based on this clock is valid on a month by month basis. GPS timing was restored in July 1997. Details of the camera and the telescope are described in Hara et

al. (1993).

The telescope was pointed in the direction of the pulsar PSR B1509−58 (right ascension $15^h13^m55^s.62$ and declination –59° 08′ 08″.9 (J2000), Taylor et al. 1995) in May and June in 1996, from March to May in 1997 and from March to May in 1998. The pulsar (ON source) and an offset region (OFF source), having the same declination as the pulsar but different right ascension, were observed for equal amounts of time each night under moonless and usually clear sky conditions. Typically, the ON source region is observed only once in a night around transit for a few hours. Two OFF source runs are carried out before and after the ON source run. The former one covers the first half of the ON source track and the latter covers the second half. In the off-line analysis, those data obtained when a small patch of cloud was obscuring the source are omitted. At the same time, the corresponding ON (or OFF) source data were also rejected from the analysis. In addition to the weather selection, the data taken when the electronics noise produced an anomalously large trigger rate were not used in the analysis. This happened in the 1996 observations. In the 1998 data, there are many nights which have a large difference of the event rate between the ON and OFF source regions, which is thought to be due to the presence of thin dew on the reflecting mirror. Data taken under these conditions were also omitted. The durations of selected observations after these procedures are 26^h30^m , 32^h08^m and 21^h14^m for the 1996, 1997 and 1998 (both ON and OFF) data, respectively. These data are used for the analysis in this paper.

Observations were carried out under different instrumental conditions in each year. During the 1996 observations, the reflectivity of the mirror was estimated to be $\simeq$ 45%. We recoated the mirror in October 1996 by vacuum evaporation of aluminium at the Anglo Australian Observatory. As a result, the reflectivity of the mirror increased to about 90%. As the reflectivity was improved, the threshold energy of our telescope was lowered.

For the 1997 observations, the threshold energy, defined here as the energy at which a differential photon flux with an assumed differential spectral index of 2.5 is maximized in the Monte Carlo calculations, was estimated to be 1.9 TeV, compared to 4.5 TeV before the recoating. By the 1998 observations, the reflectivity had decreased to $\simeq 70\%$, corresponding to a threshold energy of 2.5 TeV. In these estimations, the selection effect of the analysis described in the next section is also taken into account. In the Monte Carlo calculation, we assumed that the observations were made at a zenith angle of 30°, which was close to the average value for our observations on PSR B1509−58.

The observation times and threshold energies are summarized in Table 1, and as well, the analysis results are shown.

EDITOR: PLACE TABLE 1 HERE.

3. Analysis and Results

3.1. Analysis method

At the beginning of each run, the ADC pedestal and gain for each PMT were measured. To calibrate the gain, a blue LED located at the center of the mirror is used to illuminate the PMTs uniformly. The pedestal value is subtracted from the ADC value and any variations in the PMT gains were normalized using the LED calibration data. PMTs whose TDC value corresponded to a pulse arrival time within ± 30 nsec of the shower plane were regarded as 'hit ' tubes and used to calculate image parameters. After omitting some hit tubes which were isolated or which had ADC values less than one standard deviation above the pedestal value, the conventional image parameters (Hillas 1985) were calculated. (In the 1996 data, a fifth of the PMTs at the bottom in the camera were omitted from analysis

to avoid the effect of electronics noise. This makes the threshold energy higher and the effective area smaller. This effect is included in calculating the threshold energy and the flux upper limit.)

The parameter ranges determined from Monte Carlo simulations to optimize the gamma-ray signals are : $0^\circ.60 < \mathit{distance} \leq 1^\circ.30$, $0^\circ.04 < \mathit{width} \leq 0^\circ.09$, $0^\circ.10 < \mathit{length} \leq 0^\circ.40$, $0.35 < \mathit{concentration} \leq 0.70$ and $\alpha \leq 10^\circ$. These ranges are slightly narrower than those used in case of the Vela analysis (Yoshikoshi et al. 1997). The upper limit of α, 10°, is adopted assuming the source is a point-like. Two orientation parameters, α and *distance*, are defined with respect to the assumed source position in the field of view. In this paper, this is fixed at the pulsar position except in the spatial analysis discussed in Section-3.4. To avoid the effect of incomplete images near the edge of the camera, images with centroids located at greater than $1^\circ.05$ from the center of the camera were also rejected. We also required that the number of hit tubes (N_{hit}) must be ≥ 5 and the total number of photo-electrons contained in an image ($N_{p.e.}$) must be ≥ 40 to be able to obtain good image parameters and select only air shower induced events. The upper limit of $N_{p.e.}$ is large enough to accept all real events with large numbers of photo-electrons. In Table 1, the numbers of events in the raw data and selected are presented. We can find a large difference between ON and OFF in the raw data. The main reasons of the difference in number are the electronics noise in the 1996 data and the existence of the optically bright stars (M_V = 4.1 and 4.5) in the field of view in the 1997 data, where the reflectivity of the mirror was the largest. However, the numbers match well after the selection of air shower events. For all the three years' data analyses we applied the same criteria as described above.

3.2. Results of the image analysis

The distributions of the orientation angle (α) after all other cuts were applied are shown in Figure 1.

EDITOR: PLACE FIGURE 1 HERE.

Although there was no statistically significant excess of the ON source counts over the OFF source seen in the 1996 data, the 1997 data shows an excess at $\alpha \leq 10°$ with a statistical significance of 4.1σ. This excess may indicate the presence of a VHE gamma-ray signal from the source. The additional use of the *asymmetry* parameter showed an excess in the positive (gamma-ray–like) domain, though not at a level which would have increased the overall significance of the excess. More careful study would be necessary in use of this third-moment parameter for the source near the Galactic Center, where the night-sky background level is high. In the 1998 data, we find a small excess in the ON source counts, however, the statistical significance is only 1.4σ at $\alpha \leq 10°$. Hereafter, we regard the 1996 and 1998 results as non-detections of the VHE gamma-ray signal and treat the 1997 result as a marginal detection. The corresponding upper limits and flux are calculated as,

$$F_{99.5\%}(E \geq 4.5\,\mathrm{TeV}) \leq 1.9 \times 10^{-12}\ \mathrm{cm}^{-2}\ \mathrm{s}^{-1}$$

$$F(E \geq 1.9\,\mathrm{TeV}) = (2.9 \pm 0.7) \times 10^{-12}\ \mathrm{cm}^{-2}\ \mathrm{s}^{-1}$$

$$F_{99.5\%}(E \geq 2.5\,\mathrm{TeV}) \leq 2.0 \times 10^{-12}\ \mathrm{cm}^{-2}\ \mathrm{s}^{-1}$$

for 1996, 1997 and 1998 results, respectively. Here, a differential energy spectral index of 2.5 is assumed. The upper limits and the errors in the flux are estimated based on the numbers of the observed counts. We note that in our calculation of the upper limits the difference of the counts between ON and OFF are also taken into account following the formula introduced by Helene (1983). So the 1998 flux upper limit becomes higher than

that from completely null result. If we change the assumption of the differential energy spectral index over the range 2.5 $\pm$ 1.0, the corresponding threshold energies are estimated to change by $\sim \mp 30\%$. Instrumental uncertainties also affect the estimation of the threshold energies. We estimate the systematic error in determining the absolute threshold energies to be about 40$\sim$50%. However, because almost all of the systematic errors behave in the same way for the three years' observations, the uncertainty of the relative threshold energy is smaller than this value.

3.3. Consistency and Stability

The positive indication is obtained only from the lowest threshold energy observation. But the derived flux and two flux upper limits require neither variability of the source nor a very soft spectral index, that is, the results from the three years are consistent with each other assuming stable emission with a Crab-like spectral index ($\sim$ 2.5) or the harder index (1.8) expected by du Plessis et al. (1995). We also divided the 1997 data into separate new moon periods to check on consistency. The results are shown in Table 1. Each month's result has a marginal positive effect on the final result. The excess counting rate is stable during the three observation seasons within the statistical errors.

3.4. Spatial analysis

PSR B1509−58 and its surrounding environment are complex and there are indications from X-ray data that non-thermal phenomena possibly occur over an extended area of this remnant. So it is possible that the gamma-ray–like signal in the 1997 data is not from a point source at the pulsar position but from some other region near the pulsar. Therefore we have carried out a source search in the $2^\circ \times 2^\circ$ field of view centered on the pulsar

position. To do this, we shifted the position of the assumed source over a grid of points around the pulsar and repeated the analysis at each point to obtain the excess counts in the α distribution. The resultant map of the significance is shown in Figure 2.

EDITOR: PLACE FIGURE 2 HERE.

The peak of the excess is found at $0^\circ.1$ south-west from the pulsar. But when we consider the degrees of freedom of the search, the significance at this maximum should be reduced. And also, from a Monte Carlo calculation, where the observed counts of signal and background are taken into account, we estimated that the precision to determine the source position is $0^\circ.10$ at the 1σ level. We conclude, therefore, that the position of the excess is consistent with the pulsar position within the statistics of our observations.

3.5. Periodicity analysis

The recorded arrival times of the gamma-ray–like signals ($\alpha \leq 10^\circ$ after all the image cuts) were converted to the Solar System Barycenter arrival times using the solar system ephemeris based on epoch 2000 (DE200) (Standish, 1982). We then carried out a phase analysis with the phase parameters summarized in Table 2 (Manchester et al. 1998). Because Nel et al. (1990) pointed out a possibility of a light curve with triple peaks in the TeV energy range, we applied the H-test (de Jager, Swanepoel and Raubenheimer 1989) to obtain the statistical significance. The virtue of the H-test lies in the fact that it requires no assumptions about bin size and bin location and is also independent of the shape of the light curve. The results are summarized in Table 3.

EDITOR: PLACE TABLE 3 HERE.

The results of 1997 are divided into separate observational periods (months), because GPS timing information was not available in 1997 as mentioned in Section-2. The relative arrival time of the events is calculated for the 1997 data from the time of the crystal clock, having a constant drift rate relative to the GPS clock. The H-statistics and the corresponding probabilities against a uniform distribution are shown in Table 3. No evidence for the 150 ms periodicity is found in any of the observation seasons. To calculate the flux upper limit for the pulsed emission, we used the formula given by de Jager (1994). This formula combines the observed counts (N) and pulsed fraction (p) through a parameter, χ, as, $\chi = p\sqrt{N}$. When the H-statistic is considered as a non-detection of periodicity, χ giving 3 σ upper limit of p is expressed as,

$$\chi_{3\sigma} = (1.5 + 10.7\delta)(0.174H)^{0.17+0.14\delta} exp\left[(0.08 + 0.15\delta)\left\{log_{10}(0.174H)\right\}^2\right]$$

Here, H is the value of the H-test as shown in Table 3. (For H<0.3 we should take H=0.3 in calculating $\chi_{3\sigma}$.) δ is the duty cycle of the pulse profile. In case of PSR B1509−58, we assumed δ to be 0.3 using the X-ray observation by Kawai et al. (1991). The 3σ upper limits for the pulsed VHE gamma-ray emission are also shown in Table 3.

4. Discussion

Our observations can be summarized as follows : (1) In the observations with the lowest detection threshold energy, a 4.1σ excess of gamma-ray–like events is found. Null results in the observations of the other years (when the detection threshold energies were higher) are not in conflict with this marginal positive result : neither variability of the source nor an especially soft energy spectrum needs to be invoked. (2) From the result in the 1997 observations, there is no evidence of a variability on a monthly time-scale during three observation seasons. (3) In the 1997 data, the peak emission source position is

shifted slightly to the south-west direction from the pulsar position. However, considering the statistical error including the real event numbers observed, this is consistent with the pulsar position. (4) The periodicity of the events modulated with the radio pulsar period is studied. We found no evidence of the 150 ms pulsar periodicity using the H-test in any of the observations for three years.

The statistical significance of the 1997 excess, 4.1σ, is too small to claim as the detection of a VHE gamma-ray source, however, it is sufficiently suggestive to allow discussion supposing the excess was due to a VHE gamma-ray signal. With this scheme the simplest and most straightforward explanation can be made assuming that the emission is found from the pulsar nebula surrounding the pulsar. VHE gamma-ray emission from a pulsar nebula is usually considered as a result of inverse Compton scattering by relativistic electrons. From the emission processes of synchrotron and inverse Compton radiations, a simple equation, $\frac{\dot{\mathrm{E}}_{\mathrm{synch}}}{\dot{\mathrm{E}}_{\mathrm{iC}}} = \frac{\epsilon_{\mathrm{B}}}{\epsilon_{\mathrm{ph}}}$, can be obtained. Here $\dot{\mathrm{E}}_{\mathrm{synch}}$ and $\dot{\mathrm{E}}_{\mathrm{iC}}$ are the luminosities through synchrotron radiation (mainly resulting in quanta in the X-ray energy range) and inverse Compton scattering (mainly producing VHE gamma-rays), respectively, and ϵ_{B} and ϵ_{ph} are the energy densities of the magnetic field and the target photons for inverse Compton scattering at the emission region. Assuming isotropic emission of both X-rays and gamma-rays, $\frac{\dot{\mathrm{E}}_{\mathrm{synch}}}{\dot{\mathrm{E}}_{\mathrm{iC}}}$ can be equated to $\frac{\mathrm{F}_{\mathrm{synch}}}{\mathrm{F}_{\mathrm{iC}}}$. Here $\mathrm{F}_{\mathrm{synch}} = 7.2 \times 10^{-11}$ ergs cm^{-2} s^{-1} $(0.1 - 2.4\,\mathrm{keV})$ as given by Trussoni et al. (1996) and $\mathrm{F}_{\mathrm{iC}} = 2.7 \times 10^{-11}$ ergs cm^{-2} s^{-1}, obtained by integrating the 1997 flux above 1.9 TeV assuming a differential spectral index of 2.5. (The corresponding luminosity at the pulsar, L_{iC}, is 6.2×10^{34} ergs s^{-1} assuming the pulsar distance of 4.4 kpc. That is 0.34% of the pulsar rotating energy loss.) If the 3 K Microwave Background Radiation (MBR) is the only target of the inverse Compton radiation, *i.e.*, $\epsilon_{\mathrm{ph}} = \epsilon_{3\mathrm{K}} = 3.8 \times 10^{-13}$ ergs cm^{-3}, one obtains $\epsilon_{\mathrm{B}} = 1.0 \times 10^{-12}$ ergs cm^{-3}. This, then, leads to a value for the magnetic field strength B $\simeq$ 5 μG. Considering the large uncertainties in the arguments above, this value agrees well with the previously estimated value of

B $\simeq$ 7 μG, from the equipartition of energy between the particles and the magnetic field (Seward et al. 1984). According to the prediction of du Plessis et al. (1995), our result corresponds to a magnetic field strength of B $\simeq$ 5 μG. These three estimated values of the magnetic field agree very well with each other.

An alternative source of the target photons is the IR source IRAS 15099−5856, known to be positionally coincident with the pulsar (Arendt 1991). Du Plessis et al. (1995) estimated that the contribution from the IR photons to the VHE gamma-ray flux would be at the same level as that from the 3 K MBR. However the association between IRAS 15099−5856 and the pulsar is uncertain. In case that the IRAS source found at 25μm supplies the target photon for the inverse Compton process, the resultant VHE gamma-ray spectrum is expected to be softer than that made from the 3 K MBR. This is because the critical energy of the parent electrons in the Klein-Nishina cross section is $\sim$ 6 $\times$ 10^{12} eV against 25μm IR radiation while it is $\sim$ 10^{15} eV for the 3 K MBR. Therefore, the VHE gamma-ray spectrum should have a rapid softening over the TeV energy range. To understand the association of this IRAS source, detailed spectral measurements with future observations are required as well as the X-ray observations discussed below.

While our observations do not place any interesting limit on the spectral index, the very hard spectrum predicted by du Plessis et al. (1995) should be discussed. Their prediction was based on the observational results of the X-ray spectrum which showed a hardening of the index in the energy range below a few keV (photon index $1.4^{+0.4}_{-0.2}$ below 4 keV while 2.15±0.02 between 2 keV and 60 keV). However, recent X-ray observations do not confirm this hardening. The photon indices obtained in the wide X-ray energy band are consistent with a value around 2.2 (Trussoni et al. 1996; Tamura 1997; Marsden et al. 1997) though the error of the ROSAT result is large. To discuss the synchrotron spectrum in detail, we need information from radio observations. But, even with the recent high resolution

observations, a radio pulsar wind nebula has not been discovered (Gaensler et al. 1998).

The upper limits set to the periodic signal in this paper are one order of magnitude below the previously reported flux in the same energy band (Nel et al. 1992). Although Nel et al. reported upper limits from observations after 1988, our results should provide a far stricter limit on models. The VHE pulsed emission is in conflict with the observed cut-off around 10 MeV as predicted by the polar-cap model. To explain the VHE pulsed emission, an additional hard component, probably outer-gap emission, is required. Future observations by GLAST may reveal the existence of this component and studies of its flux and spectral variability may hint at large variability in the VHE range. The flux of the transient VHE pulsed emission reported in 1985, $F(E \geq 1.5\,\mathrm{TeV}) = (3.9 \pm 0.9) \times 10^{-11}\ \mathrm{cm}^{-2}\ \mathrm{s}^{-1}$, would make this source the brightest known VHE gamma-ray source in the southern hemisphere. We could detect this kind of activity even with short duration monitoring. Semi-simultaneous monitoring of this pulsar with the future large IACT arrays in the southern hemisphere (CANGAROO-III, HESS) and GLAST would be of great interest if the pulsar were to display such an active phase in the future.

Finally, it is notable that, unlike the other pulsar nebulae detected at VHE energies, PSR B1509−58 is not firmly detected by *EGRET* onboard the *CGRO* satellite. In contrast, this pulsar and its surroundings show a variety of the non-thermal phenomena as introduced in Section-1. A comparison of nonthermal X-ray emission with VHE gamma-ray emission is becoming very useful in the search for VHE gamma-ray sources and study of their environment. Combined with the recent studies of pulsar nebulae (Kawai and Tamura 1996), the new generation of the Imaging Atmospheric Čerenkov Telescopes (e.g. Matsubara et al. 1997) will result in an improved understanding of pulsar nebulae and particle acceleration. The CANGAROO II 7m telescope started observations at Woomera in mid-1999. From new observations with a lower energy threshold, we will be able to

measure the gamma-ray spectrum precisely and obtain a better estimation of the physical parameters, especially the magnetic field strength, in pulsar nebulae.

This work is supported by a Grant-in-Aid in Scientific Research from the Japan Ministry of Education, Science, Sports and Culture, and also by the Australian Research Council. We would like to thank to Dr. R. N. Manchester who provided us the latest radio ephemeris data on the pulsar. We are grateful to the AAO staffs in the recoating work of the 3.8m mirror. The receipt of JSPS Research Fellowships (JH, AK, TN, GPR, KS, GJT and TY) is also acknowledged. Finally, we thank the anonymous referee whose comments helped us improve the manuscript.

Table 1. Summary of the observations and the analysis results. The number of events in the ' After noise reduction' column are those remaining after the N_{hit} and $N_{p.e.}$ cuts are applied to obtain the number of air shower events. Flux upper limits for the 1996 and 1998 data are calculated as a 99.5% confidence level. For the 1997 data, the results in each newmoon season are also presented with the excess counts per minute.

Observation Period	Time (min)	Threshold Energy (TeV)	Number of Events Recorded	After noise reduction	After image selection	Flux or Upper Limit ($\times 10^{-12} cm^{-2} s^{-1}$)
1996 ON	1590	4.5	91622	16111	170	<1.9
OFF	1590		99948	17297	169	
1997 ON	1928	1.9	367689	106624	1388	2.9
OFF	1928		282156	106772	1180	
1998 ON	1274	2.5	89752	26543	345	<2.0
OFF	1274		90002	26705	309	
						(excess/min)
March 1997 ON	345		73742	19440	261	0.10±0.06
OFF	345		62193	19610	227	
April 1997 ON	598		101909	33504	426	0.12±0.05
OFF	598		82334	33610	381	
May 1997 ON	985		192038	53680	701	0.13±0.04
OFF	985		137629	53552	572	

Table 2. Pulsar timing data (from radio observation) used in the periodicity analysis (Manchester et al. 1998).

Parameter	Value
Validity range (MJD)	50114 – 51094
ν_0 (s^{-1})	6.6244525661182
$\dot{\nu}_0$ (s^{-2})	-6.73155 $\times$ 10^{-11}
$\ddot{\nu}_0$ (s^{-3})	1.95 $\times$ 10^{-21}
t_0^{geo} (MJD)	50604.000000816

Table 3. Results of the periodicity analysis. The H-test statistics for each year are shown. Because of the GPS clock problem (see text), the 1997 data are divided into three observation seasons. Chance probabilities P(>H) are calculated against a uniform light curve (no periodicity). The corresponding 3σ flux upper limits are also shown.

Observation	H-test		flux upper limit
Period	H	P(>H)	$(\times 10^{-12} cm^{-2} s^{-1})$
1996	3.55	0.24	1.7
March 1997	6.37	0.08	5.2
April 1997	0.61	0.78	2.6
May 1997	0.84	0.71	2.1
1998	3.85	0.21	1.5

REFERENCES

Arendt, R. G., 1991, AJ, 101(6), 2160

Bowden, C. C. G. et al., 1993, Proc. 23rd Internat. Cosmic Ray Conf., Calgary, 1, 294

Cheng, K. S., Ho, C. and Ruderman, M., 1986, ApJ, 300, 500

Chadwick, P. M. et al., 1997, Proc. 25th Internat. Cosmic Ray Conf., Durban, 3, 189

de Jager, O. C., Swanepoel, J. W. H. and Raubenheimer, B. C., 1989, A&A, 221, 180

de Jager, O. C., 1994, ApJ, 436, 239

de Jager, O. C. et al., 1996, ApJ, 457, 253

du Plessis, I. et al. 1995, ApJ, 453, 746

Gaensler, B. M. et al., 1998, MNRAS, 305, 724

Hara, T. et al., 1993, Nucl. Inst. Meth. Phys. Res. A, 332, 300

Harding, A. K., 1990, Nucl. Phys. B, 14A, 3

Harding, A. K., Baring, M. G. and Gonthier, P. L., 1997, ApJ, 476, 246

Helene, O., 1983, Nucl. Inst. Meth. Phys. Res., 212, 319

Hillas, A. M., 1985, Proc. 19th Internat. Cosmic Ray Conf., La Jolla, 3, 445

Kawai, N. et al., 1991, ApJ, 383, L65

Kawai, N. and Tamura. K., 1996, in 'Pulsars: Problems and Progress', ASP Conference series Vol. 105, eds. S. Johnston, M. A. Walker and M. Bailes, 367

Kifune, T. et al., 1995, ApJ, 438, L91

Kuiper, L. et al., 1999, A&A, 351, 119

Manchester, R. N., Tuohy, I. R. and D'Amico, N. 1982, ApJ, 262, L31

Manchester, R. N. et al., 1998, the Australian Pulsar Timing Archive, http://www.atnf.csiro.au/Research/pulsar/psr/archive/

Marsden, D. et al., 1997, ApJ, 491, L39

Matsubara, Y. et al., 1997, in 'Towards a Major Atmospheric Čerenkov Detector - V', Kruger, ed. de Jager, O. C., 447

Nel, H. I. et al., 1990, ApJ, 361, 181

Nel, H. I. et al., 1992, ApJ, 398, 602

Seward, F. D. and Harnden, F. R. 1982, ApJ, 256, L45

Seward, F. D. et al. 1984, ApJ, 281, 650

Standish, E. M., 1982, A&A, 114, 297

Tamura, K. et al. 1996, PASJ, 48, L33

Tamura, K., 1997, private communication

Tanimori, T. et al., 1994, ApJ, 429, L61

Taylor, J. H. et al. 1995, Princeton ftp service; http://pulsar.princeton.edu/pulsar/

Thompson, D. J. et al. 1994, ApJ, 436, 229

Torii. K. et al. 1997, ApJ, 489, L145

Trussoni, E. et al. 1996, A&A, 306, 581

Vacanti, G. et al., 1991, ApJ, 377, 467

Weekes, T. C. et al., 1989, ApJ, 342, 379

Yoshikoshi, T. et al., 1997, ApJ, 487, L65

This manuscript was prepared with the AAS LaTeX macros v4.0.

Fig. 1.— Distributions of the α parameter after all other image cuts. The solid and dashed lines in upper figures show the ON source and OFF source results, respectively. The bottom figures represent the ON–OFF counts of the upper figures.

Fig. 2.— The contour map of the significance around the pulsar position in the 1997 data. North is to the top of the figure, and west is to the right. The field of view is $2^\circ \times 2^\circ$ and the pulsar position is indicated by the cross. The distance from the pulsar position to the peak of the excess (SW from the pulsar) is $0^\circ.1$ and is consistent with the pulsar position within the source localization error, which is indicated by the circle.

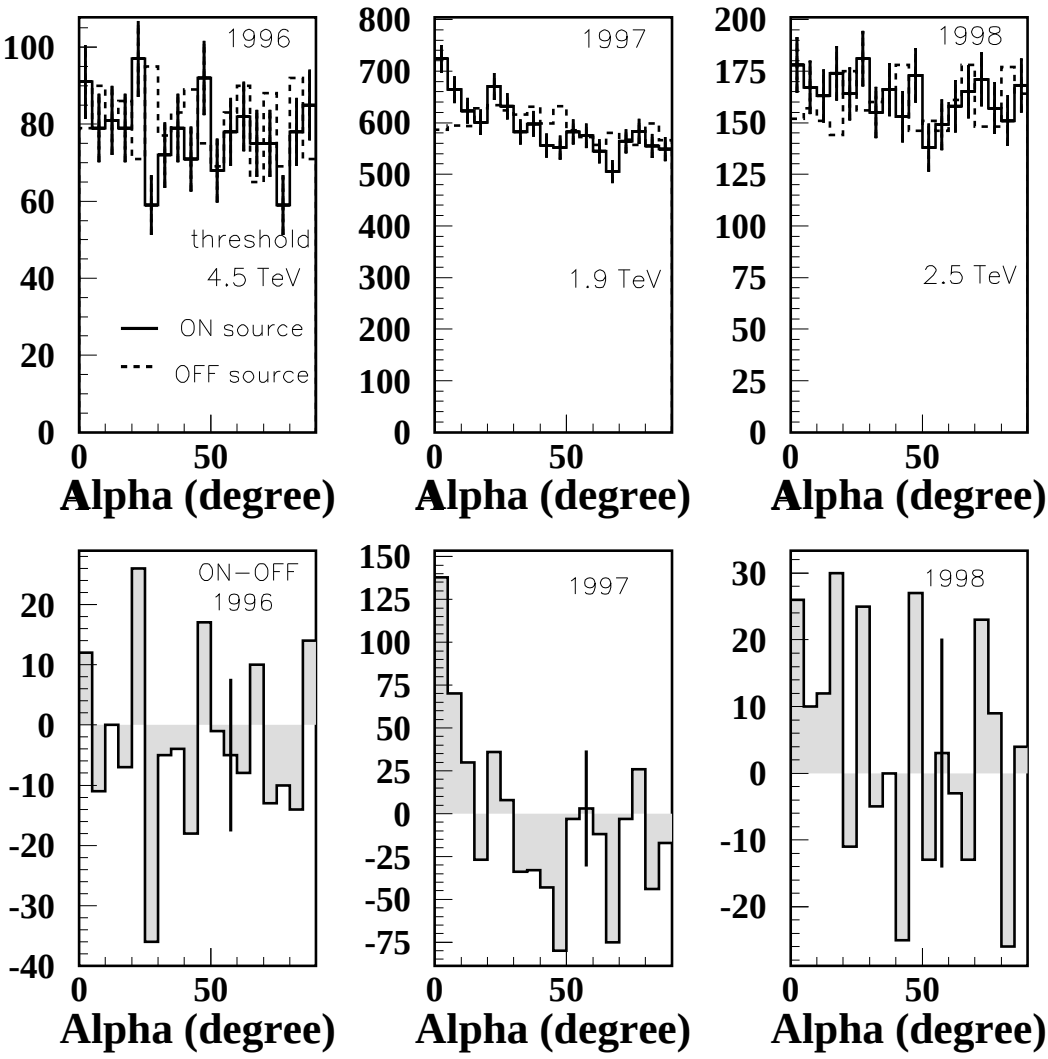
1996
threshold
4.5 TeV
ON source
OFF source
1997
1.9 TeV
1998
2.5 TeV
ON−OFF
1996
1997
1998
Alpha (degree)
Alpha (degree)
Alpha (degree)
Alpha (degree)
Alpha (degree)
Alpha (degree)

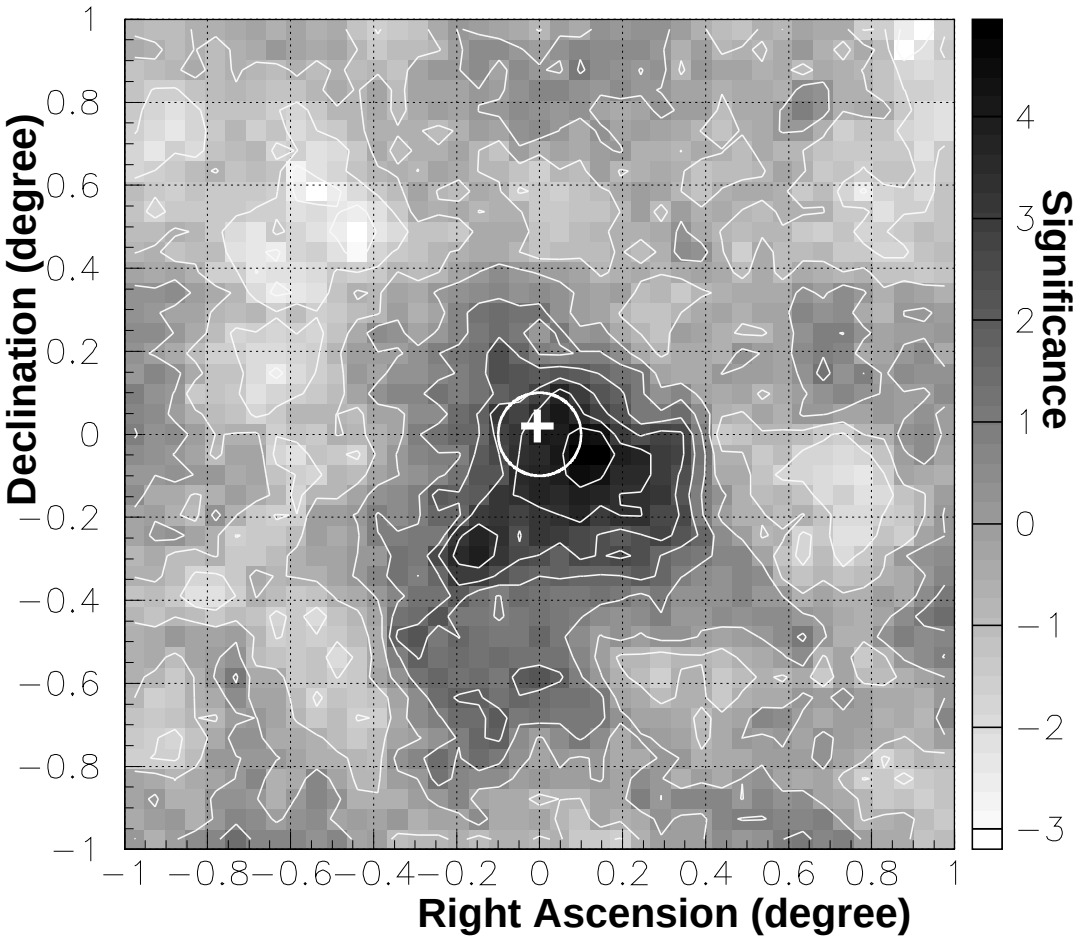
Declination (degree)
Right Ascension (degree)
Significance
1
0.8
0.6
0.4
0.2
0
−0.2
−0.4
−0.6
−0.8
−1
−1 −0.8 −0.6 −0.4 −0.2 0 0.2 0.4 0.6 0.8 1
4
3
2
1
0
−1
−2
−3